Modification of the Physical-mechanical Properties of Bamboo-plastic Composites with Bamboo Charcoal after Hydrothermal Aging

Qi Chen,[a,b] Rong Zhang,[a,*] Daochun Qin,[a] Zexu Feng,[b] and Yangao Wang [b,*]

The physical-mechanical properties of bamboo-polyethylene composites (BPCs) change depending on the environmental temperature and exposure to moisture during outdoor use. In this study, the water absorption, density, mechanical properties, and wear rate of the composites were tested after immersion in water, and four water temperatures were examined. Bamboo charcoal (BC) was used to improve the properties of the BPCs after hydrothermal aging. The composites were improved because of the strong interfacial interactions between the BC and polymers. The experimental results showed that the water diffusion rate accelerated as the water temperature increased. The BC reduced the water absorption at all of the water temperatures and the diffusion coefficient at temperatures above 39 °C. The wear rate of the composites first increased, and then decreased as the water temperature increased. The density and flexural properties decreased with an increased hydrothermal aging temperature. Overall, hydrothermal aging decreased the water resistance and mechanical properties. Additionally, these effects were enhanced as the water temperature increased, but were countered by the incorporation of the BC.

Keywords: Bamboo-plastic composites; Bamboo charcoal; Hydrothermal aging; Wear rate; Mechanical properties

*Contact information: a: International Centre for Bamboo and Rattan, Key Laboratory of Bamboo and Rattan and Technology of State Forestry Administration, Beijing, China, 100102; b: Sichuan Agricultural University, Key Laboratory of Wood Industry and Furniture Engineering, Chengdu, China, 611130; *Corresponding author: WangYangao_sicau@163.com; zhangrong@icbr.ac.cn*

INTRODUCTION

Wood-plastic composites (WPCs) are manufactured by combining natural plant fibers, such as wood, bamboo, sisal (Joseph *et al*. 2002), coir (Espert *et al*. 2004), and flax (Stamboulis *et al*. 2000), with currently produced thermoplastics. The composites are processed by hot pressing (Zhou *et al*. 2015), extrusion (Xian *et al*. 2015(a)), or injection molding (Kuo *et al*. 2009). These composites have been widely used in nonstructural construction, furniture, and transportation applications (Xian *et al*. 2015(b)) because of their low cost, recyclability, and environmental compatibility (Aydemir *et al*. 2015). In most of these applications the material is exposed to a high water content, as well as frequent temperature changes. The water absorbed by the plant fibers in the composites can affect the dimensional stability, mechanical properties (Tissandier *et al*. 2014), and resistance to biological decay (Yildiz *et al*. 2005).

For WPCs used outside, the physical-mechanical properties change depending on the environmental temperature and humidity. Many studies have investigated the effects of hydrothermal aging on the properties of these materials. Tamrakar and Lopez-Anido (2011) investigated the water absorption and mechanical properties of WPCs immersed in water at different temperatures (21 °C, 45 °C, and 70 °C) and found that the water absorption at equilibrium increased as the temperature increased. The mechanical properties decreased after immersion in water. This phenomenon occurred because the wood fibers swelled, which caused the polymer matrix to yield locally and

decreased the adhesion between the wood fibers and polymers. The mechanical properties increased slightly for the specimens that were first immersed at 21 °C and then dried again, which was possibly because the different amount of water absorbed caused the wood fibers to swell to a different degree. Hence, less microcracks were produced when the water absorption was lower. Espert *et al*. (2004) found that a higher content of natural plant fibers resulted in a greater decline in the mechanical properties after immersion in water. Their scanning electron microscopy (SEM) results showed that the pectin layer and microfibrils were degraded after immersion in 50 °C water, and this behavior was attributed to the decline in the mechanical properties. Lin *et al*. (2002) investigated the changes in the mechanical properties of WPCs after water immersion and found that the flexural strength, flexural modulus, and impact strength increased after immersion in 23 °C water, but decreased upon immersion in 60 °C and 100 °C water. Most existing studies have focused on the properties of WPCs during the water immersion process (Stark 2001; Espert *et al*. 2004). Few studies have examined the effects of wetting and re-drying WPCs.

Bamboo charcoal (BC) is a well-suited reinforcement material for polymers (Ho *et al*. 2015) and WPCs (Li *et al*. 2014) because of its high porosity, high resistance to moisture, and high strength, among other factors. The strong interfacial adhesion between BC and polymers could increase the strength and decrease the water absorption of WPCs (You and Li 2014). The BC can also improve the thermal stability of WPCs and bamboo-plastic composites (BPCs) (Li *et al*. 2014; Zhu *et al*. 2016) and reduce the hydrophilicity of BPCs (Chen *et al*. 2016). Despite the many benefits that BC exhibits, its use to improve the properties of WPCs after hydrothermal aging has not yet been investigated.

Bamboo-plastic composites are manufactured using remainders from bamboo processing as a natural plant fiber that is then blended with a thermoplastic matrix material. Fewer studies have focused on BPCs than WPCs (Xian *et al*. 2015b). In this study, bamboo fiber (BF) and low-density polyethylene (LDPE) were used to manufacture composites, and BC was used as the reinforcing material to improve the properties of BPCs after hydrothermal aging. The effects from four different hydrothermal aging temperatures on the BPCs were investigated, and the Arrhenius equation was used to predict the water diffusion coefficient at different immersion temperatures. Additionally, the mechanical properties and wear rates of the specimens after immersion in water and re-drying were investigated in this study. By investigating the influence of hydrothermal aging on the BPCs and BPCs modified with BC (BPC-BCs) it is possible to determine the damage mechanisms of hot water on BPCs and made BPCs a wider used filed such as the bathroom.

EXPERIMENTAL

Materials

The BF (less than 40 mesh size) was purchased from Weihua Spices Factory (Guangdong, China). The LDPE (density = 0.913 g/cm^3) was purchased from SuZhou JoeShun Plastic Co. Ltd. (Suzhou, China). The BC was purchased from QuZhou Nine Wave E-commerce Co. Ltd. (Zhejiang, China). The vinyltrimethoxy silane coupling agent (A-171) was purchased from NanJingYouPu Chemical Co. Ltd., and the acetic acid and ethanol (analytically pure) were supplied by Beijing Chemical Works (Beijng, China).

Methods

Preparation of the specimens

The BPC formulation used for testing was a BF:LDPE ratio of 6:4 (mass fraction), and the BPC-BC formulation was a BF:LDPE:BC ratio of 5:4:1 (mass fraction). These formulations were set according to the authors' previous study, which reported that BPC-BC exhibited the best mechanical properties when the BC content was 8% to 12% (Chen *et al*. 2016). The BF was treated with 4 wt.% of the coupling agent. The coupling agent was dissolved in ethanol with an appropriate amount of acetic acid to adjust the pH of the solution to 4.5 to 5.5, and then the solution was heated to 60 °C for 10 min. The mixture solution was sprayed onto the BF uniformly at room temperature, and the mass ratio of the solution to BF was 1:1. Then, the treated BF was dried in an oven at 100 °C ± 1 °C for 24 h to reach a constant weight. All of the BF, LDPE, and BC materials were dried in an oven to reach a constant weight, and then premixed in a malaxator (NH-1, Guancheng Machine Co., Ltd., JiangSu, China). The mixing temperature of the materials was 50 °C, and the mixing time was 30 min. Afterwards, the mixture was transferred to a mold and hot-pressed (8 MPa) at 150 °C for 30 min. Finally, the composites were removed from the mold after reducing the temperature to 35 °C at a rate of approximately 22 °C/min using cold water.

Water absorption

Water absorption tests were conducted according to ASTM D570-98 (2005). Five samples from each set were tested using deionized water, and the dimensions of the specimens were 45 mm (length) × 45 mm (width) × 4.5 mm (thickness). All of the specimens were placed in an oven at 50 °C ± 1 °C for 24 h, and then immersed in deionized water at 23 °C, 45 °C, 70 °C, and 100 °C. To record data, the specimens that were immersed at 23 °C were removed from the water, wiped off using blotting paper, weighed, and placed back in the water. The specimens immersed at higher temperatures (45 °C, 70 °C, and 100 °C) were removed from the water and maintained in room temperature water for 5 min to cool the samples down. Then, blotting paper was used to wipe off the surface water, and the samples were weighed. The tests were conducted after 1 h, 4 h, 9 h, 16 h, and 25 h *et al.* until 600 h, and this continued until the procedures were completed.

The percentage of water absorbed (M) was calculated by Eq. 1,

$$M\,(\%) = (m_t - m_0) / m_0 \times 100\% \quad (1)$$

where m_0 (g) and m_t (g) are the masses of the composite before and after immersion in water for various times, respectively. The diffusion behavior was theoretically distinguished from the shape of the initial part of the absorption curve using Eq. 2 (Comyn 1985),

$$\frac{M_t}{M_\infty} = k \cdot t^n \quad (2)$$

where M_t is the water content (*%*) at a specific time (*t, h*) and M_∞ is the maximum water content (*%*). When the value of n is close to 0.5, the absorption process can be described by Fick's law of diffusion, and the diffusion coefficient (D) can be calculated with the following equation,

$$D = \frac{\pi}{16 M_\infty^2}\left[\frac{M_t}{\sqrt{t}/h}\right] \quad (3)$$

where h is the thickness *(mm*) of the composite sheet (when dry) and D denotes the diffusion coefficient.

Density

All specimens were conditioned at 23 °C with 50% relative humidity for two weeks after hydrothermal aging. The density of all the specimens was tested using a solid densimeter using the water displacement method (DH-120E, Taiwan Matsu Haku Scientific Instrument Co., Ltd., Xiamen, China). Before starting the test, all specimens were oven-dried at 103 °C ± 1 °C until the change in weight was 2 mg or less over a 3-h period. The results were averaged for at least five specimens, and the dimensions of the specimens were 10 mm × 10 mm × 4.5 mm.

Mechanical properties

All specimens were conditioned at 23 °C with 50% relative humidity for two weeks after hydrothermal aging. The flexural strength (MOR) and flexural modulus (MOE) were tested following the standard ASTM D790-10 (2010) using a universal testing machine (Instron 5582, Instron, Norwood, USA), and the dimensions of the samples were 90 mm × 15 mm × 4.5 mm. The notched impact test was conducted using an impact-type testing machine (XJJ-5, Kecheng Testing Machine Co., Ltd., Chengdu, China) as specified by the standard ASTM D6110-10 (2010), and the dimensions of the samples were the same as those of the samples used for the flexural properties test. The reported values were the average of at least five specimens.

Wear properties

The wear properties were measured in accordance with standard GB/T 3960-2016 (2016) using an abraser machine (5155 Abraser, Taber Industries, New York, USA). The loading on the specimens was 7.5 N, the test time was 2000 s, and the speed was 72 rpm. The results were expressed as the average of three specimens, and the dimensions were 100 mm × 100 mm × 4.5 mm. The wear rate was calculated by Eq. 4,

$$\omega = \frac{\Delta m}{\rho \times F \times L} \quad (4)$$

where ω is the wear rate ($cm^3/(N \cdot m)$), Δm is the loss of the wear quality (g), ρ is the density of the specimen (g/cm^3), F is the loading (N), and L is the slide distance of the steel ring (m).

Morphology characterization

Micrographs of the specimens were obtained using SEM (JEOLJSM-6310F, JEOL, Tokyo, Japan) with an accelerating voltage of 7.0 kV. The specimens were coated with a layer of platinum by vacuum evaporation before testing.

Statistical analysis

SPSS 18.0 software (SPSS Inc., Chicago, USA) was used to analyze the data. Analysis of variance (ANOVA) techniques were used, and significant differences between the variables were investigated at the 95% confidence level.

RESULTS AND DISCUSSIONS

Water Absorption Behavior

The weight of each sample was measured at a specific time to characterize the water behavior. The samples were tested after 1 h, 4 h, 9 h, 16 h, and 25 h because the initial parts of the water absorption *versus* √t plots are fairly linear (Tamrakar and Lopez-Anido 2011). The water adsorption percentages are shown in Fig. 1. Nearly all of the specimens absorbed water rapidly during the first stage, and then the absorption rate decreased until the equilibrium condition was reached and the weight of the

specimens became constant. The water absorption of the BPC-BC decreased by between 4% and 6% for all of the test immersion temperatures compared with the BPC. Since LDPE is a hydrophobic material and it cannot absorb water (Li *et al*. 2014), the increase in the water absorption was attributed to the BF. BF and the gaps between BF and LDPE provide the channels available for water absorption in BPC, so the BF content decrease would decrease the number of channels. Besides, BC could block the gaps between the BF and LDPE, which also would decrease the channels available for water in BPC-BC (Chen *et al*. 2016). The maximum water absorption of the BPC at 23 °C was 17.6%. The absorption increased to 20.2% at 45 °C, and declined to 19.5% at 70 °C, but within a margin of error that made the difference between 45 °C and 70 °C statistically insignificant. In contrast, the maximum water absorption of the BPC-BC increased as the immersion temperature increased. A few authors have reported that the maximum water absorption increased with the increasing immersion temperature, while others have reported the opposite (Joseph *et al*. 2002; Espert *et al*. 2004; Tamrakar and Lopez-Anido 2011). It was hard to determine whether this difference was caused by the immersion temperature because these composites were produced using different manufacturing technologies and contained different fiber species and contents.

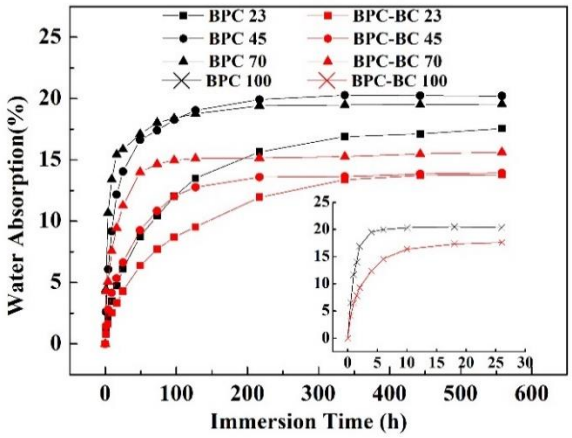

Fig. 1. Water absorption curves of the BPC and BPC-BC at different immersion temperatures

Table 1. Diffusion Curve Fitting Parameters for the BPC and BPC-BC

Specimen	*n*	*k*	M_∞ (%)	*D* (m^2/s) × 10^{-12}
BPC 23	0.5621	0.0567	17.56	0.95
BPC 45	0.6272	0.0967	20.21	1.86
BPC 70	0.5713	0.1439	19.54	2.56
BPC 100	0.4342	0.5259	20.35	7.11
BPC-BC 23	0.5365	0.0561	13.78	1.09
BPC-BC 45	0.4695	0.1049	13.91	1.68
BPC-BC 70	0.5263	0.1362	15.63	2.23
BPC-BC 100	0.5021	0.3528	17.61	5.21

The absorption process was different for different immersion temperatures. With an increasing temperature, the rate of diffusion increased, and the time required to reach the maximum water absorption was shortened. The period to reach the maximum water absorption was 6 h for the BPC at 100 °C, but was 337 h at 23 °C. The increased water temperature increased the motion of the water molecules, and thus the rate of diffusion increased. Table 1 shows the *n* and *k* values obtained using Eq. 2. The value of *n* was close to 0.5; thus, the Fick's diffusion model was used to describe the diffusion of water in the BPC and BPC-BC (Zabihzadeh *et al*. 2010). The water diffusion coefficients for the composites are shown in Table 1. Similar results were also obtained by many other studies (Espert *et al*. 2004; Adhikary *et al*. 2008; Zabihzadeh

et al. 2010; Tamrakar and Lopez-Anido 2011). As was expected, the value of *D* increased with the increasing immersion temperature. This result was also obtained by Espert *et al*. (2004) and Tamrakar and Lopez-Anido (2011).

Because the absorption behavior followed Fickian diffusion, an exponential Arrhenius-type equation could be used to predict the diffusion coefficient at any temperature. This equation is expressed below (Comyn 1985),

$$D(T) = D_0 \exp\left[-\frac{E_a}{R \cdot T}\right] \quad (5)$$

where $D(T)$ (m^2/s) is the diffusion coefficient at immersion temperature T (K), D_0 is the permeability index (m^2/s), E_a is the activation energy for diffusion (kJ/mol), and R is the universal gas constant (8.314 J/K/mol). From Eq. 5, Eq. 6 was derived as follows,

$$\ln D(T) = \ln D_0 - \frac{E_a}{R} \cdot \frac{1}{T} \quad (6)$$

Thus, E_a/R and D_0 could be determined from the slope and intercept of Eq. 6, respectively (Fig. 2). The Arrhenius-type relation could be used to predict the diffusion coefficient at any temperature using the experimental data. Thus, Eq. 5 was rewritten as Eqs. 7 and 8. The addition of the BC into the BPC reduced the apparent activation energy for diffusion.

$$D_{BPC}(T) = 9.7111 \times 10^{-9} \exp\left[-\frac{2743.53}{T}\right] \quad (7)$$

$$D_{BPC-BC}(T) = 1.4380 \times 10^{-9} \exp\left[-\frac{2147.36}{T}\right] \quad (8)$$

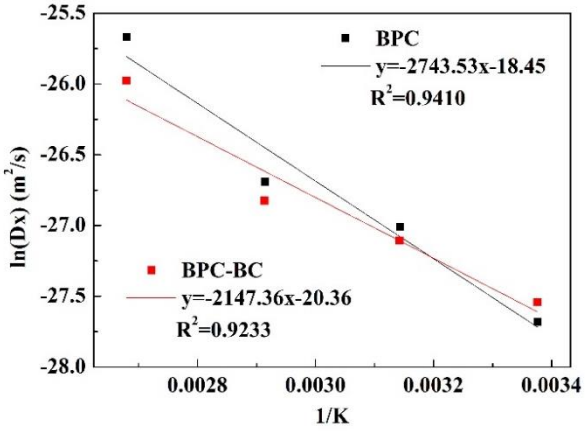

Fig. 2. Arrhenius plot for the BPC

Figure 3 shows the diffusion coefficient as a function of the temperature using Eqs. 7 and 8 and the experimental data. When the temperature was lower than 39 °C, the diffusion coefficient of the BPC was slightly lower than that of the BPC-BC. At temperatures above 39 °C, the diffusion coefficient of the pure BPC was higher than that of the BPC-BC. This difference became wider as the temperature increased further. Thus, BC reduced the diffusion of water when the immersion temperature was high. Yang *et al*. (2005) reported that strong interfacial adhesion between the fibers and polymers could reduce the coefficient of thermal expansion. The LDPE could permeate the pores of the BC and interact strongly with the BC (Chen *et al*. 2016). Thus, the thermal expansion coefficient of the BPC-BC was lower than that of the BPC, and fewer gaps were formed in the BPC-BC after the composite was heated. Finally, this interaction resulted in a decreased diffusion coefficient for the BPC-BC.

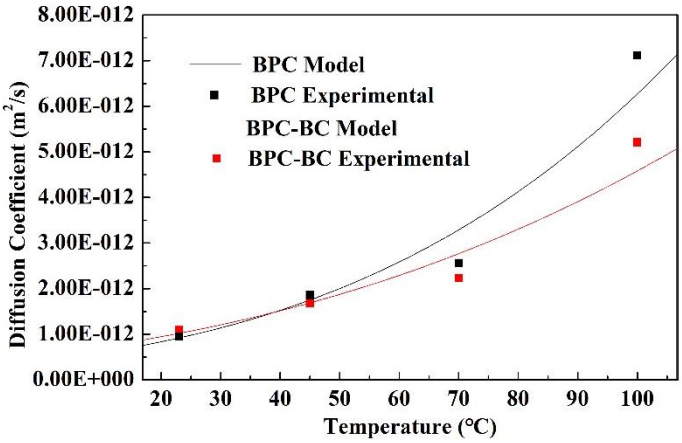

Fig. 3. Diffusion coefficient as a function of the temperature

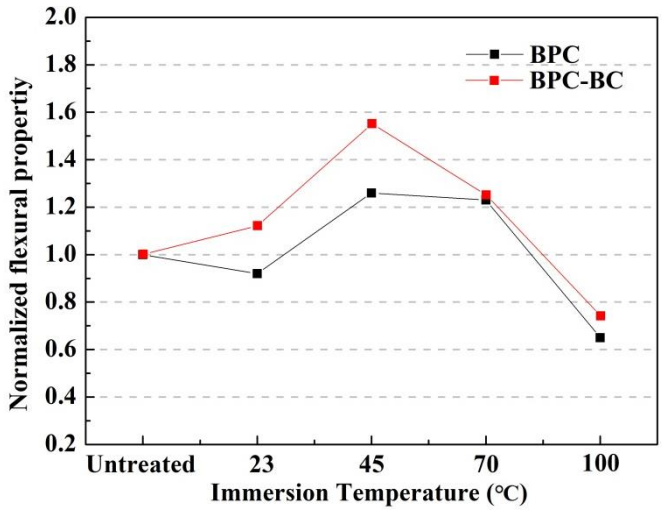

Fig. 4. Effect of the immersion temperature on the wear loss of the BPC and BPC-BC

Wear Loss

Table 2 displays the mechanical and physical properties for all specimens. The effect of the hydrothermal aging temperature on the wear rates of the BPC and BPC-BC is also given. Figure 4 shows the evolution of wear loss as a function of the temperature, which was expressed as the ratio between the wear loss upon immersion at different temperatures and the wear loss of the untreated specimen. The results indicated that the wear rate of both the BPC and BPC-BC first increased and then decreased with an increase in the water temperature. The maximum wear loss was found at the water temperature of 45 °C. The wear loss increased after immersion in water because the BFs absorbed water and expanded, which created larger gaps between the BFs and LDPE. Compared with the untreated specimen (Fig. 5a), the specimen that was immersed (Fig. 5b) clearly exhibited many gaps around the BFs. It was concluded that the BFs were more easily delaminated from the BPC. Therefore, compared with the worn surface of the untreated BPC (Fig. 5c), the BPC immersed at 45 °C (Fig. 5e) showed more damage and more delamination on the worn surface. It was observed that the wear loss increased after immersion.

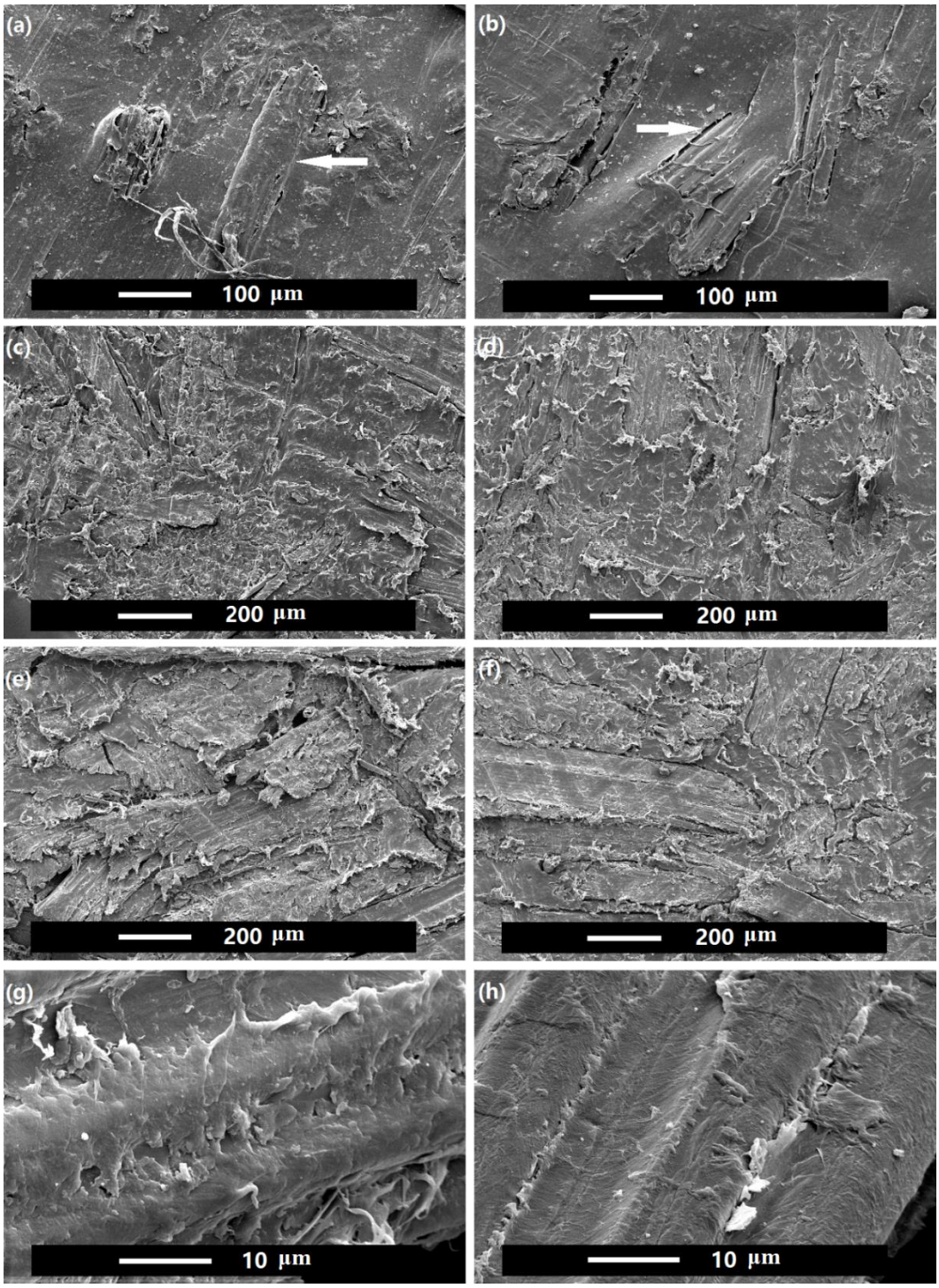

Fig. 5. SEM micrographs of: the flat surfaces of the BPC without treatment (a) and after immersion in 45 °C water (b); the worn surfaces of the BPC without treatment (c), BPC-BC without treatment (d), BPC after immersion in 45 °C water (e), and BPC after immersion in 100 °C water (f); and fracture surfaces of the BPC without treatment (g) and after immersion in 100 °C water (h)

In general, when the water temperature increased, both LDPE and BFs would absorb more heat and expand further, so the gaps between LDPE and BF became bigger after two weeks condition of the specimens. This made the BFs are more easily delaminated, and the wear loss is increased. However, when the temperature was above 70 °C, the wear rate did not increase, but instead decreased (Table 2 and Fig. 4). Figure 5f shows the worn surface of the BPC treated at 100 °C.

Table 2. Physical-mechanical Properties of the BPC and BPC-BC after Hydrothermal Aging

Specimen	Wear Rate (%) × 10^{-5}		Density (g/cm^3)		MOR (MPa)		MOE (MPa)		Impact Strength (kJ/m^3)	
	BPC	BPC-BC	BPC	BPC-BC	BPC	BPC-BC	BPC	BPC-BC	BPC	BPC-BC
Untreated	4.20 (0.45) b	3.57 (0.75)ab	1.050 (0.008) a	1.093 (0.009) a	13.0 (0.6) a	14.6 (0.1) a	1013 (72) a	1304 (54)a	9.04 (0.54) bc	8.12 (0.39) ab
23 °C	4.72 (0.59) b	3.30 (0.89) bc	1.038 (0.004) b	1.052 (0.009) b	10.5 (0.2) b	12.4 (0.2) b	467 (16) b	656 (28) b	10.77 (0.38)a	8.43 (0.38) a
45 °C	6.53 (0.81) a	4.48 (0.28) a	1.006 (0.003) c	1.050 (0.006) b	9.1 (0.1) c	10.7 (0.2) cd	342 (25) c	554 (77) c	9.47 (0.36) bc	7.65 (0.46) b
70 °C	5.27 (0.61) b	4.38 (0.22)ab	0.991 (0.009) d	1.034 (0.005) c	7.8 (0.5) d	10.8 (0.1) c	310 (47) c	563 (28)c	9.56 (0.37) b	8.45 (0.31) a
100 °C	3.12 (0.38) c	2.31 (0.49) c	0.983 (0.012) d	1.023 (0.002) d	7.5 (0.3) d	10.5 (0.4) d	250 (19) d	564 (67) c	8.70 (0.99) c	8.50 (0.40) a

Note: The letters a,b,c,d indicate significant differences based on the Duncan's analysis of variance. The same letter represented there was no significant difference between the specimens at the significance level of 5%.

Compared with the BPC treated at 45 °C (Fig. 5e), the detachment of the BPC worn surface decreased, and little delamination was observed. The wear loss likely increased because of the loss of the pectin layer. By increasing the water temperature, hot water extractives were obtained from the BFs, and pectin is an important component in hot water extractives. Figure 5g shows the BFs of the BPC without treatment, and Fig. 5h shows the BFs of the BPC after immersion in 100 °C water. In contrast to the untreated BFs, the BFs after immersion at 100 °C lacked a pectin layer, the similar result was obtained by Espert *et al*. (2004). Some authors (Stokes *et al*. 2011; Tingting *et al*. 2014) found that pectin shows low friction when used as an additive in water, possibly because a lubricating film forms on the wear surface. Figure 6 shows that gaps were produced around the BFs after immersion, and the BFs that were immersed at a lower temperature were covered with a pectin layer. The pectin layer allowed the BFs to detach more easily from the matrix because it reduced the friction effect between the BFs and matrix. When the specimen was immersed at a higher temperature, the pectin layer was dissolved. Therefore, the BFs had stronger interactions with the matrix, and the wear rate decreased.

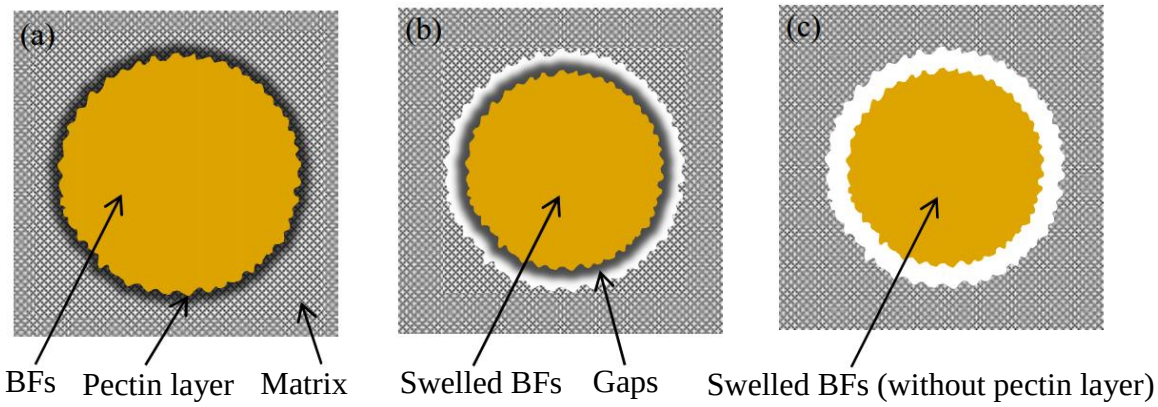

Fig. 6. Interfacial reaction mechanism of the BPC without treatment (a) and after immersion at lower (b) and higher temperatures (c)

BC was effective at reducing the wear rate of the BPC at any water temperature. There are two possible reasons for this result. First, the strong interactions between the BC and polymer (Li *et al*. 2014; Chen *et al*. 2016; Zhu *et al*. 2016) increased the difficulty of delaminating the polymer from the surface. Figure 5c shows the worn surface of the BPC without treatment, and Fig. 5d shows the worn surface of the BPC-BC without treatment. Both of these worn surfaces indicated that the polymer was delaminated after wear. However, the polymer was found to have delaminated more from the worn surface of the BPC than from that of the BPC-BC. The BC interacted strongly with the polymer, and these interactions decreased polymer delamination because of friction and wear, which decreased the wear rate. Second, the multiple laminated graphite planes existing in the carbon fibers endowed the fibers with a self-lubricating characteristic (Song *et al*. 2007; Lkhagvasuren *et al*. 2016; Luo *et al*. 2016). Other fibers such as chrysotile asbestos fibers or glass fibers also can be used to reinforce the wear resistance of WPCs (Luo *et al*. 2013; Zhang *et al*. 2016).

Mechanical Properties

The density of the specimens decreased as the hydrothermal aging temperature increased (Table 2). The density of the untreated BPC decreased from 1.050 g/cm^3 to 1.038 g/cm^3 after immersion in 23 °C water because the BF in the matrix expanded after immersion (Espert *et al*. 2004) and shrank after re-drying, which created many gaps. This mechanism increased the volumes of the specimens, and so the density

decreased. When the hydrothermal aging temperature increased to 100 °C, the density decreased to 0.983 g/cm^3. This change was attributed to several factors, such as the increase in the expansion rate of the BF, removal of bamboo extractives, and degradation of the BF *via* the hydrolysis mechanism during hydrothermal aging (Espert *et al*. 2004). The BC filled the gaps between the LDPE and BFs (Chen *et al*. 2016), and so the density of the BPC-BC was higher than that of the BPC at any water temperature.

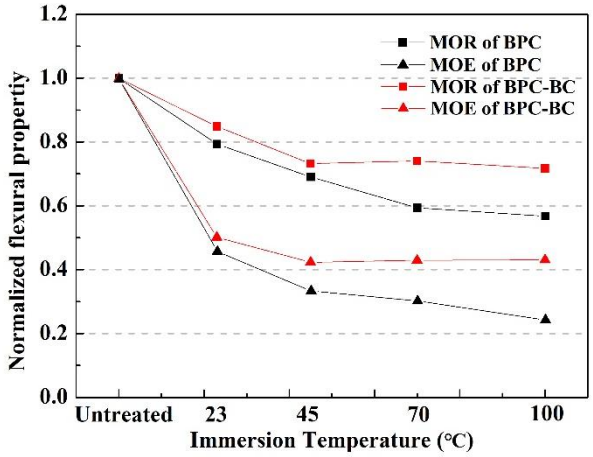

Fig. 7. Effect of the immersion temperature on the flexural properties of the BPC and BPC-BC

Table 2 reports the flexural properties, and Fig. 7 shows the evolution of the flexural properties as a function of the temperature and expressed as the ratio between the specimens after immersion at different temperatures and the untreated specimens. The results indicated that the MOR of the specimens was smaller than that of the specimens that were untreated after immersion in water and decreased further as the hydrothermal aging temperature increased. The MOR of the specimens was decreased by 19.2% after immersion at 23 °C. When the immersion temperature was increased to 100 °C, the MOR decreased by 42.3%. The decrease in the MOR could have been related to the decrease in the density of the composites. The BC could have enhanced the BPC whether the specimens were hydrothermally aged or not for the following reasons. First, the LDPE had strong interactions with the BC because it could permeate into the porous BC in a molten state (Li *et al*. 2014). Additionally, the BC was able to reinforce the BPC by filling the gaps between the BFs and LDPE (Chen *et al*. 2016). However, when the hydrothermal aging temperature was below 45 °C, the MOR of the BPC-BC decreased as the temperature increased, and when the immersion temperature was 70 °C and 100 °C, the MOR remained almost constant. The strong interactions between the LDPE and BC reduced the thermal expansion coefficient of the composite (Yang *et al*. 2005; Chen *et al*. 2016). Therefore, the smaller thermal expansion coefficient of the BPC-BC led to the formation of fewer gaps after heating the composites and resulted in a constant MOE value for the BPC-BC above 45 °C. These results suggested that the BC might prevent the strength of the BPC from decreasing after aging in water at a high temperature.

The trend of the MOE was similar to that of the MOR, but it showed a greater degree of reduction after immersion (Fig. 7). The main reason for this may have been that the interaction between the BFs and LDPE became weaker after expansion and shrinking. The softening of the desorbed zones of the cellulose microfibrils might have caused this decrease (Lin *et al*. 2002; Akil *et al*. 2014). The MOE of the BPC-BC was higher than that of the BPC after hydrothermal aging at all of the tested temperatures. The MOE increased because the BC could restrict the motion of the polymer chains, which may have permeated the pores of the BC (Chen *et al*. 2016).

Table 3. Comparison of the Flexural Properties and Impact Strength for Different Immersion Temperatures from Previous Studies

Temperature (°C)	Wood Fiber	Polymer	Molding Method	Immersion Time	MOR		MOE		Impact Strength		Reference
					Before Immersion (MPa)	After Immersion (%)	Before Immersion (MPa)	After Immersion (%)	Before Immersion (kJ/m^3)	After Immersion (%)	
21 to 23	15% wood fiber	PP	Injection	72 h / 420 h#	56	3.57[a]	1900	40.53[a]	3.29	0.4	Lin *et al*. (2002)
					65.5	3.82[b]	2000	33.50[b]			
	30% cellulose	PP	Hot press	Water-saturated	-	-	1260	-40.48	-	-	Espert *et al*. (2004)
	40% wood fiber	PP	Injection	Water-saturated	46	-21.74	3600	-36.11	-	-	Stark (2001)
	46% pine	PP	Extrusion	Water-saturated	22.5	0.44[c]	3700	-43.24[c]	-	-	Tamrakar and Lopez-Anido (2011)
					32.1	-30.53[d]	4300	-55.81[d]			
					22.5	8.00[c]*	3700	-32.43[c]*			
					32.1	-21.18[d]*	4300	-41.86[d]*			
	60% BF	LDPE	Hot press	Water-saturated	13	-19.23*	1013	-53.90*	9.04	19.14*	-
45 to 50	30% cellulose	PP	Hot press	Water-saturated	-	-	1260	-34.92	-	-	Espert *et al*. (2004)
	46% pine	PP	Extrusion	20 d	22.5	-1.78[c]	3700	-43.24[c]	-	-	Tamrakar and Lopez-Anido (2011)
					32.2	-9.94[d]	4300	-46.51[d]			
	60% BF	LDPE	Hot press	Water-saturated	13	-30.00*	1013	-66.24*	9.04	0.05*	-
60 to 70	15% wood fiber	PP	Injection	72 h / 240 h#	56	-3.57[a]	1900	-15.79[a]	3.29	0.16	Lin *et al*. (2002)
					65.5	-4.58[b]	2000	-10.00[b]			
	30% cellulose	PP	Hot press	Water-saturated	-	-	1260	-35.71	-		Espert *et al*. (2004)
	46% pine	PP	Extrusion	Water-saturated	22.5	-8.00[c]*	3700	-51.35[c]*	-	-	Tamrakar and Lopez-Anido (2011)
					32.2	-31.99[b]*	4300	-55.81[d]*			
	60% BF	LDPE	Hot press	Water-saturated	13	-40.00*	1013	-69.40*	9.04	0.06*	-

Temperature (°C)	Wood Fiber	Polymer	Molding Method	Immersion Time	Before Immersion (MPa)	After Immersion (%)	Before Immersion (MPa)	After Immersion (%)	Before Immersion (kJ/m^3)	After Immersion (%)	-
100	15% wood fiber	PP	Injection	72 h / 240 h[#]	56	-3.57[a]	1900	-10.53[a]	3.29	0.11	Lin *et al*. (2002)
					65.5	-6.87[b]	2000	-10.00[b]			
	30% sisal	PP	Injection	7 h	-	-	753	-23.28	-	-	Joseph *et al*. (2002)
	60% BF	LDPE	Hot press	Water-saturated	13	-42.31*	1013	-75.32*	9.04	-0.04*	-

Note: [a] Results for the untreated WF, [b] Results for the treated WF, [c] Results for the WPC flange, [d] Results for the WPC web, * Results for the WPC after re-drying, [#] Immersion time was 72 h for the flexural properties and 420 h or 240h for the impact strength.

Hydrothermal aging had no significant effect on the impact strengths of the BPC and BPC-BC (Table 2). After hydrothermal aging, the specimens had a higher water content than the specimens without treatment because the new gaps were able to contain more water. The water molecules could resist the impact energy, and so the impact resistance increased (Pandian *et al*. 2014). However, the degradation of the BFs decreased the impact strength when the specimens were immersed at high temperatures. The BC could not improve the impact strength of the BPC. This result was also observed in the authors' previous study (Chen *et al*. 2016).

A comparison between the flexural properties and impact strength of WPCs at different immersion temperatures is shown in Table 3, along with the results of previous studies that used different wood fibers and molding methods. Almost all of the flexural properties of the test specimens decreased by various degrees, except for the samples in the study by Lin *et al*. (2002). The author attributed this behavior to decreased interfacial debonding and increased interfacial shear strength. In the current study, the flexural properties further decreased as the hydrothermal aging temperature increased, but similar conclusions were not reached in previous studies. These results may have been related to the high BF content, as BFs are more sensitive to hydrothermal aging than the polymer. Additionally, the flexural properties also further decreased as the wood fiber content increased with a constant immersion temperature.

Hydrothermal aging did not have a significant effect on the impact strength of WPCs. Stark *et al*. (2001) speculate this might because the swelling of fibers made it difficult to pull out from the matrix (Stark 2001; Lin *et al*. 2002). Previous studies on hydrothermal aging using WPCs mainly focused on PP. However, more polymers should be studied because, for example, polyethylene and polyvinyl chloride are also raw materials commonly used in WPCs.

CONCLUSIONS

1. In this study, the BPC and BPC-BC were aged at four different water temperatures and tested. It was found that the moisture penetration behavior followed Fick's law. When the immersion temperature was higher, the diffusion coefficient was larger. The BC reduced the water absorption at all of the water temperatures and reduced the diffusion coefficient at temperatures higher than 39 °C because the BPC-BC has a small linear thermal expansion coefficient.
2. The wear rates of the composites first increased and then decreased as the water temperature increased. Immersion in water helped the BF to dislodge from the matrix. However, a higher water temperature degraded the pectin layer and decreased the wear rate. The BC also reduced the wear rate at all of the tested temperatures because of its strong connection with the polymer and its self-lubricating characteristics.
3. The density and flexural properties of the specimens were clearly reduced after immersion and re-drying, and the decrease became sharper as the hydrothermal aging temperature increased because aging in water increased the gaps between the BF and LDPE. The BC increased the flexural properties of the BPC after hydrothermal aging, not only because of the strong interactions between the BC and polymer, but also because of the smaller thermal expansion coefficient for the BPC-BC.

ACKNOWLEDGMENTS

The authors express sincere thanks to the State Forestry Administration Key Laboratory for Bamboo and Rattan Science & Technology and Sichuan Agricultural University. This work was financially supported by the National Key Research and Development Program of China (Grant No. 2017YFD0600803) and the Fundamental Research Funds for the International Centre for Bamboo and Rattan (No. 1632017020).

REFERENCES CITED

Adhikary, K. B., Pang, S., and Staiger, M. P. (2008). "Long-term moisture absorption and thickness swelling behaviour of recycled thermoplastics reinforced with *Pinus radiata* sawdust," *Chem. Eng. J.* 142(2), 190-198. DOI: 10.1016/j.cej.2007.11.024

Akil, H. M., Santulli, C., Sarasini, F., Tirillò, J., and Valente, T. (2014). "Environmental effects on the mechanical behaviour of pultruded jute/glass fibre-reinforced polyester hybrid composites," *Compos. Sci. Technol.* 94(4), 62-70. DOI: 10.1016/j.compscitech.2014.01.017

ASTM D570-98 (2005). "Standard test method for water absorption of plastic," ASTM International, West Conshohocken, PA.

ASTM D6110-10 (2010). "Standard test method for determining the Charpy impact resistance of notched specimens of plastics," ASTM International, West Conshohocken, PA.

ASTM D790-10 (2010). "Standard test methods for flexural properties of unreinforced and reinforced plastics and electrical insulating materials," ASTM International, West Conshohocken, PA.

Aydemir, D., Kiziltas, A., Kiziltas, E. E., Gardner, D. J., and Gunduz, G. (2015). "Heat treated wood-nylon 6 composites," *Compos. Part B-Eng.* 68, 414-423. DOI: 10.1016/j.compositesb.2014.08.040

Chen, Q., Zhang, R., Wang, Y., Wen, X., and Qin, D. (2016). "The effect of bamboo charcoal on water absorption, contact angle, and the physical-mechanical properties of bamboo/low-density polyethylene composites," *BioResources* 11(4), 9986-10001. DOI: 10.15376/biores.11.4.9986-10001

Comyn, J. (1985). *Polymer Permeability*, Elsevier Applied Science Publishers, London, UK.

Espert, A., Vilaplana, F., and Karlsson, S. (2004). "Comparison of water absorption in natural cellulosic fibres from wood and one-year crops in polypropylene composites and its influence on their mechanical properties," *Compos. Part A-Appl. S.* 35(11), 1267-1276. DOI: 10.1016/j.compositesa.2004.04.004

GB/T 3960-2016 (2016). "Plastics - Test method for friction and wear of plastics by sliding (in Chinese)," Standardization Administration of China, Beijing, China.

Ho, M.-P., Lau, K.-T., Wang, H., and Hui, D. (2015). "Improvement on the properties of polylactic acid (PLA) using bamboo charcoal particles," *Compos. Part B-Eng.* 81, 14-25. DOI: 10.1016/j.compositesb.2015.05.048

Joseph, P. V., Rabello, M. S., Mattoso, L. H. C., Joseph, K., and Thomas, S. (2002). "Environmental effects on the degradation behaviour of sisal fibre reinforced polypropylene composites," *Compos. Sci. Technol.* 62(10–11), 1357-1372. DOI: 10.1016/S0266-3538(02)00080-5

Kuo, P.-Y., Wang, S.-Y., Chen, J.-H., Hsueh, H.-C., and Tsai, M.-J. (2009). "Effects of material compositions on the mechanical properties of wood-plastic composites manufactured by injection molding," *Mater. Design* 30(9), 3489-3496. DOI: 10.1016/j.matdes.2009.03.012

Li, X., Lei, B., Lin, Z., Huang, L., Tan, S., and Cai, X. (2014). "The utilization of bamboo charcoal enhances wood plastic composites with excellent mechanical and thermal properties," *Mater. Design* 53, 419-424. DOI: 10.1016/j.matdes.2013.07.028

Lin, Q., Zhou, X., and Dai, G. (2002). "Effect of hydrothermal environment on moisture absorption and mechanical properties of wood flour-filled polypropylene composites," *J. Appl. Polym. Sci.* 85(14), 2824-2832. DOI: 10.1002/app.10844

Lkhagvasuren, U., Ozawa, Y., and Kikuchi, T. (2016). "Wear and friction properties of bp/c/c composites with bamboo charcoal particles and bacterial cellulose," *Mech. Eng. J.* 3(3), 1-9. DOI: 10.1299/mej.15-00743.

Luo, J.-L., Sun, S.-W., Liu, W.-Q., Li, Q.-Y., Hu, X.-C., Gao, S., and Han, P. (2013). "Chrysotile asbestos fiber reinforced wood-plastic composite and its application performances in formwork," *Journal of Qingdao Technological University* 34, 1-5.

Luo, W., Liu, Q., Li, Y., Zhou, S., Zou, H., and Liang, M. (2016). "Enhanced mechanical and tribological properties in polyphenylene sulfide/polytetrafluoroethylene composites reinforced by short carbon fiber," *Compos. Part B-Eng.* 91, 579-588.DOI: 10.1016/j.compositesb.2016.01.036

Pandian, A., Vairavan, M., Thangaiah, W. J. J., and Uthayakumar, M. (2014). "Effect of moisture absorption behavior on mechanical properties of basalt fibre reinforced polymer matrix composites," *J. Compos.* 2014(2), 1-8. DOI:10.1155/2014/587980

Song, H.-J., Zhang, Z.-Z., and Luo, Z.-Z. (2007). "A study of tribological behaviors of the phenolic composite coating reinforced with carbon fibers," *Mater. Sci. Eng. A* 445-446, 593-599. DOI: 10.1016/j.msea.2006.09.081

Stamboulis, A., Baillie, C. A., Garkhail, S. K., van Melick, H. G. H., and Peijs, T. (2000). "Environmental durability of flax fibres and their composites based on polypropylene matrix," *Appl. Compos. Mater.* 7(5-6), 273-294. DOI: 10.1023/A:1026581922221

Stark, N. (2001). "Influence of moisture absorption on mechanical properties of wood flour-polypropylene composites," *J. Thermoplast. Compos.* 14(5), 421-432. DOI: 10.1106/UDKY-0403-626E-1H4P

Stokes, J. R., Macakova, L., Chojnicka-Paszun, A., de Kruif, C. G., and de Jongh, H. H. (2011). "Lubrication, adsorption, and rheology of aqueous polysaccharide solutions," *Langmuir*. 27(7), 3474-84. DOI: 10.1021/la104040d

Tamrakar, S., and Lopez-Anido, R. A. (2011). "Water absorption of wood polypropylene composite sheet piles and its influence on mechanical properties," *Constr. Build. Mater.* 25(10), 3977-3988. DOI: 10.1016/j.conbuildmat.2011.04.031

Tingting, T., Weixu, W., Yong, W., and Jibin, P. (2014). "Friction reducing properties of water-based lubricant of pectin affected by inorganic salt anion," *Lubr. Eng.* 12, 53-57.

Tissandier, C., Zhang, Y., and Rodrigue, D. (2014). "Effect of fibre and coupling agent contents on water absorption and flexural modulus of wood fibre polyethylene composites," in: *Proceedings of the 29th International Conference of the Polymer Processing Society*, Nuremberg, Germany, pp. 411-415.

Xian, Y., Li, H., Wang, C., Wang, G., Ren, W., and Cheng, H. (2015a). "Effect of white mud as a second filler on the mechanical and thermal properties of bamboo residue fiber/polyethylene composites," *BioResources* 10(3), 4263-4276. DOI:

10.15376/biores.10.3.4263-4276
Xian, Y., Wang, C., Wang, G., Ren, W., and Cheng, H. (2015b). "Understanding the mechanical and interfacial properties of core-shell structured bamboo-plastic composites," *J. Appl. Polym. Sci.* 133(10). DOI: 10.1002/app.43053
Yang, H.-S., Wolcott, M. P., Kim, H.-S., and Kim, H.-J. (2005). "Thermal properties of lignocellulosic filler-thermoplastic polymer bio-composites," *J. Therm. Anal. Calorim.* 82(1), 157-160. DOI: 10.1007/s10973-005-0857-5
Yildiz, Ü. C., Yildiz, S., and Gezer, E. D. (2005). "Mechanical properties and decay resistance of wood-polymer composites prepared from fast growing species in Turkey," *Bioresource Technol.* 96(9), 1003-1011. DOI: 10.1016/j.biortech.2004.09.010
You, Z., and Li, D. (2014). "Highly filled bamboo charcoal powder reinforced ultra-high molecular weight polyethylene," *Mater. Lett.* 122, 121-124. DOI: 10.1016/j.matlet.2014.01.010
Zabihzadeh, S. M., Hashemi, S. K. H., Nikoo, H. M., and Sepidehdam, S. M. J. (2010). "Influence of fungal decay on physico-mechanical properties of a commercial extruded bagasse/PP composite," *J. Reinf. Plast. Compos.* 29(11), 1750-1756. DOI: 10.1177/0731684409340596
Zhou, Y., Ning, L., Li, X., Zhang, J., Lu, Y., and He, J. (2015). "Effect of natural flake graphite on triboelectrification electrostatic potential of bamboo flour/high-density polyethylene composites," *Wood Sci. Technol.* 49(6), 1269-1280. DOI: 10.1007/s00226-015-0752-6
Zhu, S., Guo, Y., Chen, Y., Su, N., Zhang, K., and Liu, S. (2016). "Effects of the incorporation of nano-bamboo charcoal on the mechanical properties and thermal behavior of bamboo-plastic composites," *BioResources* 11(1), 2684-2697. DOI: 10.15376/biores.11.1.2684-2697

Article submitted: October 2, 2017; Peer review completed: December 5, 2017; Revised version received: December 23, 2017; Accepted: December 27, 2017; Published: January 18, 2018.
DOI: 10.15376/biores.13.1.1661-1677